RELIABLE, INTENSE, ULTRAFAST AND COMPACT GUIDED-WAVE LASER FOR CLOUD PENETRATION, REMOTE SENSING, AND ACTIVE IMAGING

Philippe Bado

CLARK-MXR, INC.
7300 W. HURON RIVER DR.
DEXTER, MI 48130

September 2000

Final Report

APPROVED FOR PUBLIC RELEASE; DISTRIBUTION IS UNLIMITED.

20020307 031

AIR FORCE RESEARCH LABORATORY
Directed Energy Directorate
3550 Aberdeen Ave SE
AIR FORCE MATERIEL COMMAND
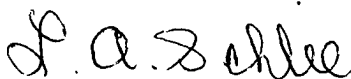**KIRTLAND AIR FORCE BASE, NM 87117-5776**

AFRL-DE-TR-2000-1079

Using Government drawings, specifications, or other data included in this document for any purpose other than Government procurement does not in any way obligate the U.S. Government. The fact that the Government formulated or supplied the drawings, specifications, or other data, does not license the holder or any other person or corporation; or convey any rights or permission to manufacture, use, or sell any patented invention that may relate to them.

This report has been reviewed by the Public Affairs Office and is releasable to the National Technical Information Service (NTIS). At NTIS, it will be available to the general public, including foreign nationals.

If you change your address, wish to be removed from this mailing list, or your organization no longer employs the addressee, please notify AFRL/DELS, 3550 Aberdeen Ave SE, Kirtland AFB, NM 87117-5776.

Do not return copies of this report unless contractual obligations or notice on a specific document requires its return.

This report has been approved for publication.

Dr. L. A. Schlie, ST
Project Manager

SYLVIA DORATO, DR-III
Chief, Tactical Laser Branch

FOR THE COMMANDER

R. EARL GOOD, SES
Director, Directed Energy

REPORT DOCUMENTATION PAGE

Form Approved
OMB No. 0704-0188

1. REPORT DATE *(DD-MM-YYYY)*	2. REPORT TYPE	3. DATES COVERED *(From - To)*
10-09-2000	Final Report	10/05/1999 – 10/03/2000

4. TITLE AND SUBTITLE
Reliable, Intense, Ultrafast and Compact Guided-Wave Laser for Cloud Penetration, Remote Sensing, and Active Imaging

5a. CONTRACT NUMBER
F29601-99-C-0044

5b. GRANT NUMBER

5c. PROGRAM ELEMENT NUMBER
65502F

6. AUTHOR(S)
Philippe Bado

5d. PROJECT NUMBER
3005

5e. TASK NUMBER
DO

5f. WORK UNIT NUMBER
BJ

7. PERFORMING ORGANIZATION NAME(S) AND ADDRESS(ES)

Clark-MXR, Inc.
7300 W. Huron River Dr.
Dexter, MI 48130

8. PERFORMING ORGANIZATION REPORT NUMBER

MXR0010

9. SPONSORING / MONITORING AGENCY NAME(S) AND ADDRESS(ES)
AFRL/DELS
3550 Aberdeen Ave SE
Kirtland AFB NM 87117-5776

10. SPONSOR/MONITOR'S ACRONYM(S)

11. SPONSOR/MONITOR'S REPORT NUMBER(S)
AFRL-DE-TR-2000-1079

12. DISTRIBUTION / AVAILABILITY STATEMENT

Approved for Public Release; distribution is unlimited

13. SUPPLEMENTARY NOTES

14. ABSTRACT
The goal of this program is to develop reliable, ultrafast, high peak-power lasers. These lasers will be used in the military for cloud penetration, reconnaissance, remote sensing, and active illumination; in the microelectronic industry for repair of photomasks and for memory yield improvement; in the automotive industry for sensors and fuel injector machining; and in the aerospace industry for turbine blade machining. We met all of our Phase I objectives. We built a fiber based front-end delivering peak power in excess of 10 MW. We demonstrated the direct write of large core waveguides. We fabricated active waveguides by direct write. We demonstrated a new non-linear Raman-Soliton compression technique. Combining these various results, we are confident that we will be able to deliver fiber lasers capable of delivering peak power in the gigawatt and ultimately the terawatt range.

15. SUBJECT TERMS
Fiber Laser, High Peak Power, Fiber Amplifier, Chirp Pulse Amplification, Non-linear Raman-Soliton Compression, Cascaded Non-linear Compression

16. SECURITY CLASSIFICATION OF:			17. LIMITATION OF ABSTRACT	18. NUMBER OF PAGES	19a. NAME OF RESPONSIBLE PERSON
a. REPORT	**b. ABSTRACT**	**c. THIS PAGE**	Unlimited	46	Dr. L.A. Schlie
Unclassified	Unclassified	Unclassified			**19b. TELEPHONE NUMBER** *(include area code)* (505) 853-3440

Standard Form 298 (Rev. 8-98)
Prescribed by ANSI Std. 239.18

Table of Contents

Figures:

Project Summary

The goal of this program is to develop reliable, compact, ultrafast, high peak-power lasers. These lasers will be used in the military for cloud penetration, reconnaissance, remote sensing, and active illumination; in the microelectronic industry for repair of photomasks, and for SRAM/DRAM (Static or Dynamic random access memory) yield improvement; in the automobile industry for sensors and fuel injector machining; and in the aerospace industry for turbine blade machining. They will also find use in the medical field.

Clark-MXR's design departs drastically from the traditional free-space cavity approach that has been the basis of all ultra-high peak power lasers built to-date. Rather we rely exclusively on optical fibers. These fibers, coupled with diode pumping, are used in chirped-pulse amplification geometry. They provide ultra-high peak powers coupled with exceptional compactness and robustness.

We met all of our Phase I objectives. We built a fiber based front-end delivering peak power in excess of 10 MW. We demonstrated the direct write of large core waveguides. We fabricated active waveguides by direct write.[1] We demonstrated a new non-linear Raman-soliton compression technique. Combining these various results we are confident that we will be able to deliver fiber lasers capable of delivering peak power in the gigawatt and ultimately terawatt range.

Note that this work has some very exciting commercial potential. Clark-MXR was able to attract funding from a venture capitalist firm. Additional funding is expected in the near future.

This program was conducted in collaboration with Professor Kim Winick of the University of Michigan.

Background Information

Today's high peak-power ultrafast lasers are bulky (tens of cubic feet), inefficient (wall plug efficiency well below 1%), water-cooled (requiring gallons per minute), and unreliable (key components with a lifetime of a few thousand hours). They require highly skilled operators and are extremely sensitive to vibrations and temperature changes. Last but not least, today's energetic femtosecond sources are unstable, even when operated in very mild environments. They constantly drift and require daily, if not hourly, realignment. Not surprisingly they are used only in R&D laboratories. Yet, femtosecond lasers can produce peak powers unmatched by any other man-made device and thus are of interest to the military and the industry at large. Over the last 20 years, hundreds of potential applications requiring femtosecond lasers have been demonstrated, yet these applications have invariably failed commercially due to the non-availability of reliable, simple, intense ultrafast sources. We do believe that this can be changed. It is the goal of this SBIR program to develop a reliable, simple, and compact energetic femtosecond source that will be of great use to the military and in industry.

The laser industry record shows that traditional designs (*i.e.* free-space designs based on mirror-bound optical cavities) just cannot achieve this goal: although femtosecond sources have substantially improved since their first appearance in the late 70's, they have not been able to move out of the R&D market. Fundamental design changes are necessary before these unique tools are able to play a role in the military and in industry.

Clark-MXR has demonstrated over the last two years that fiber lasers can provide the reliability and compactness demanded to move femtosecond technology out of the R&D world. We have shown that ultrafast devices based on guided-wave optics are far less sensitive to vibrations and shocks than traditional designs. We have also shown that guided-wave components naturally lend themselves to very compact designs. We have shown that efficiency can be increased significantly using the long-interaction region provided by guided-wave optics. These demonstrations have resulted in the recent commercialization of robust femtosecond fiber oscillators. Others have confirmed the commercial potential of guided-wave femtosecond sources.

Material constraints have so far restricted these commercial lasers to low energy levels (Peak powers limited to a few tens of kW). Above this level, non-linear effects (self-phase modulation, Raman stimulation, etc.) can play havoc with the pulse temporal and spatial structure. These constraints have been partially alleviated using the chirped pulse

2

amplification approach: the pulse peak power has been pushed to the Megawatt range (this latest development is not yet commercially available).

TABLE 1: This Program's sources compared to traditional femtosecond sources

	Traditional intense femtosecond sources	This program
Architecture	Chirped pulse amplification	Chirped pulse amplification
Oscillator	Self-modelocked Ti: Sapphire	Single-mode erbium-doped fiber
Oscillator pump	Argon laser	Communication grade diode laser
Pulse stretcher	Bulk optics, reflective gratings	Single mode fiber with Bragg gratings
Pre-amplifier	None	Single-mode erbium-doped fiber
Amplifier	Ti:Sapphire regenerative amplifier	Ultra-large single-mode fiber
Amplifier pump	Frequency-doubled Nd:YAG or Nd:YLF	Diode lasers
Compressor	Bulk optics, reflective gratings	Transmission gratings
Size	4' x 8'	2' x 1'
Operating Parameters	100 fs, 1 kHz, 1 mJ	10 fs, 100 Hz, 10 mJ
Electrical consumption	60-80 kW	< 1 kW
Water consumption	7-10 gal/min	None
Warm-up time	Never fully stable	10-20 minutes

We believe that recent advances in macroscopic scale waveguide design, photonic crystal fiber, and waveguide manufacturing can significantly alleviate today's material limitations, opening the way for the demonstration and ultimately the commercialization of Gigawatt- and potentially Terawatt-range robust, simple and compact ultrafast lasers.

Phase I Technical Objectives

The goal of this SBIR program is to design a compact, robust, high intensity femtosecond laser that will ultimately be used in harsh environments (military and heavy-industry). Our design relied primarily on single-mode optical fibers. In that context the main questions that needed to be answered during the Phase I of this program were: what is the maximum peak power that can be expected from fiber-based ultrafast lasers, and how short a pulse can we generate with fiber lasers? We also answered a second set of questions related to the manufacturing of large core waveguide in preparation for our Phase II.

Fiber-based ultrafast lasers: Maximum peak power?

Fiber-based ultrafast laser oscillators have been commercially available for a few years. Several manufacturers offer devices designed for the communication industry. For this market, very low peak power is generally required (tens of Watts), thus these devices are of limited interest for this program. In contrast the fiber lasers manufactured by Clark-MXR (See Figure 1) or IMRA America (a subsidiary of Toyota) are designed to provide peak power in the tens of kW range.

FIGURE 1: ErF, a kW range fiber laser manufactured by Clark-MXR
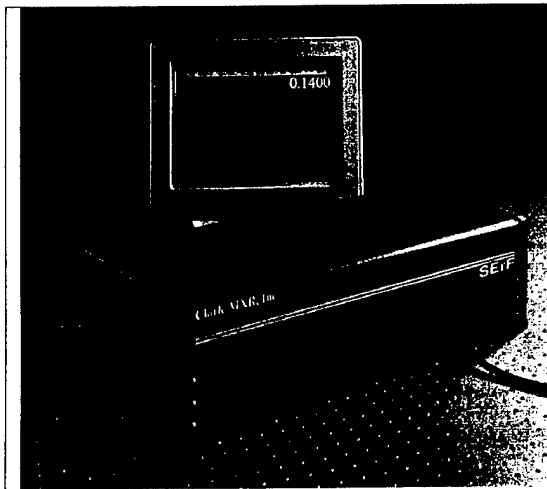
This first generation commercial ultrafast laser was developed 3 years ago in collaboration with MIT using SBIR funding. A new version using a telecommunication grade diode as the primary pump is now in manufacturing. Approximately 50 units have been delivered so far.

The generation of higher peak-powers in optical fibers cannot be done directly. Non-linear effects (self-phase modulation, Raman stimulation, etc.) combine to destroy the temporal and spatial structure of the pulse. These problems are found in all femtosecond lasers, but they are more prevalent in fiber lasers due to the prolonged confinement of the

4

optical energy in a spatially constricted area. A typical telecommunication-grade single-mode fiber has an active area of approximately 10 micron^3 (10^{-7} cm^2). A 100-fs, 1 nJ pulse (peak power =10^4 W) propagating along that single mode fiber will generate intensities of 10^{11} W/cm^2. This is at or above the threshold for numerous non-linear effects in glass fiber.[2]

The generation in fiber-based lasers of peak power exceeding the tens of kW range is feasible, but it does involve more complex approaches. The most common technique to control these non-linear material effects is the chirped pulse amplification[3,4] (CPA) geometry (see Figure 2), a technique invented by Dr. Mourou – a co-founder of Clark-MXR.

FIGURE 2: The CPA concept

Ultrafast, high energy pulse

Femtosecond low energy pulse

Long, high energy pulse

Long, low energy pulse
100 -1000 ps

Oscillator → Stretcher → Amplifier(s) → Compressor →

#990104B
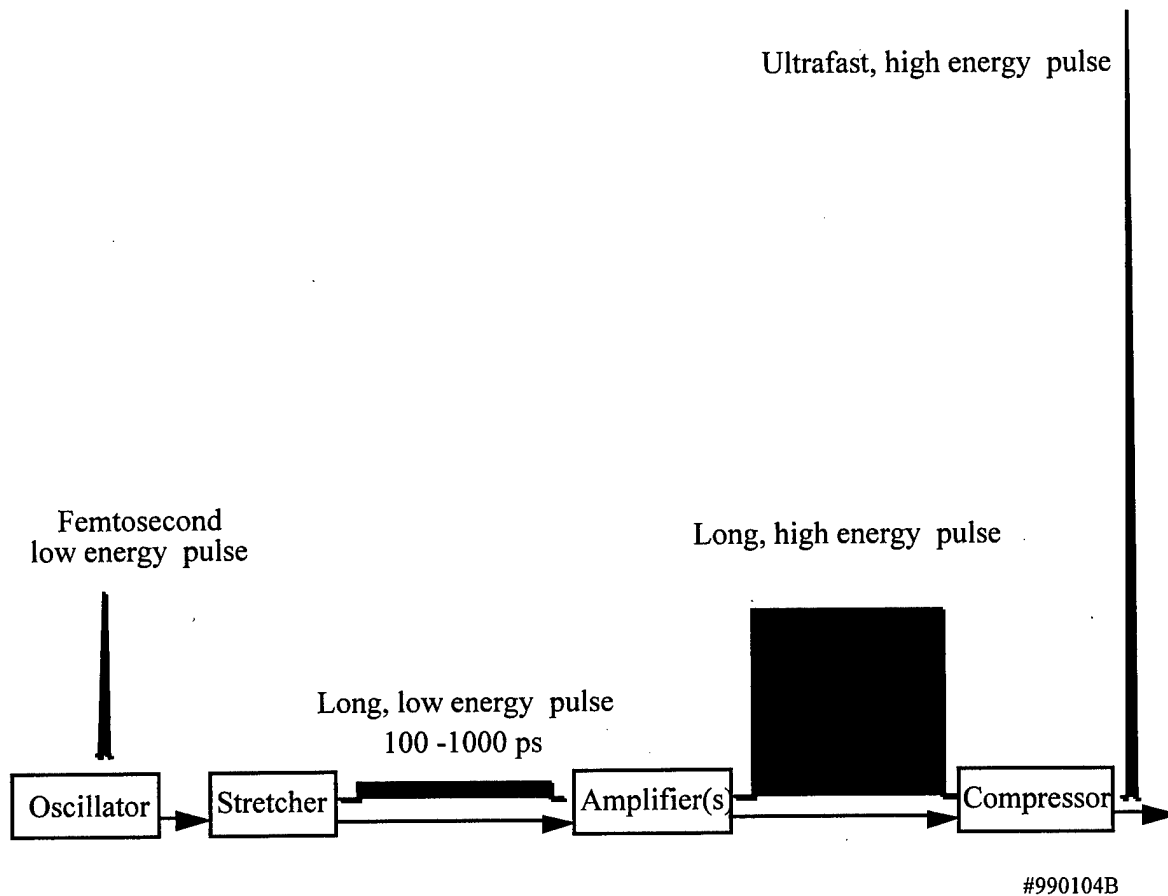
In a typical CPA design the pulse is stretched thousand-fold in time prior to amplification, allowing for an equivalent increase in the peak power. The CPA approach is so powerful that all commercial high intensity femtosecond sources are based on it. While conceptually simple, the CPA architecture calls for numerous subsystems, thus potentially making the overall system unreliable, susceptible to drift, and generally difficult to operate.

The principle underlying CPA has been tested at various levels in fiber-based laser systems. [5,6] it has been shown that the CPA approach is generally compatible with fiber-based lasers and can enhance peak power. Fiber lasers based on this geometry should be capable of providing peak powers in the Megawatt range, and they should regain their unique compactness and robustness. This type of fiber laser is not commercially available at this time. Figure 3 shows one of the preferred embodiments. This type of laser (without the compressor section) will be used at the front-end of our system. Note that by itself this laser is already of commercial interest and Clark-MXR intends to manufacture this type of product.

FIGURE 3: Fiber-based CPA system

fiber oscillator, 1550 nm **<100 fs,100 pJ, kW** ref: 990105A **Fiber-based Pulse Stretcher** **fiber amplifier, 1550 nm** **1000 ps, 10 μJ, 10 kW** **Compressor, 1550 nm, <100 fs,** **10 μJ, 100 MW**	This energetic fiber-based ultrafast source uses the chirped pulse amplification architecture to reliably generate peak power in the multi-Megawatt range. The pulses from the oscillator are frequency chirped prior to being amplified. The pulses are compressed down to their initial duration after compression. The pulse stretcher will be fiber-based. A repetition rate selector will be inserted prior to, or just after the fiber stretcher. Extreme robustness will be the key feature of this ultrafast source.

With the CPA approach, the larger the stretching ratio, the higher the resulting peak power. In traditional CPA systems, stretching ratios in excess of 10^5 have been demonstrated.[7] So far more modest stretching ratios have been the norm in fiber-based systems.[8]

To further increase the peak power generated by femtosecond fiber-based systems, several groups have tested large-area single-mode fibers.[9] This approach seems to be limited to one order of magnitude improvement over conventional single-mode fibers. It does however illustrate that significant gain can be achieved if one could use a very large area single-mode waveguide (See following Section). In one or two cases multimode-fibers operated in a single mode configuration have been used.[10] This latest approach, which

requires careful alignment, is probably not compatible with the harsh environment expected in the Air Force applications.

Phase I Work Plan

This program's tasks were divided between two teams. The primary team, based at Clark-MXR, was lead by Dr. Mark Dugan, assisted by Dr. Ali Said. The second team, based on the Ann Arbor North campus of the University of Michigan, was directed by Professor Kim Winick.

Eight tasks were defined. Tasks 1 to 3 are concerned with maximizing the peak and reducing the pulse duration from the fiber-based front-end. Tasks 4 to 7 are related to our long-term goal of increasing further the peak power in large core waveguides. Task 8 was related to reporting activities.

TASK 1: Study maximum stretching ratio for fiber CPA

Phase I Task Definition:

As explained in the previous section, the CPA stretching ratio has to be optimized in order to maximize the peak power provided by the fiber section of our laser. Stretching optical pulses is relatively simple, but doing it in a way that can be later perfectly reversed (in the compressor) requires careful design. This problem is compounded by the very large bandwidth called for in our program. We will study various ways to optimize this stretching ratio while assuring a clean recompression. Some preliminary work is required (See Task 1 A). The fiber-stretcher that is called for in our design is likely to incorporate imbedded gratings (Bragg gratings). Picosecond to nanosecond pulse stretching with Bragg gratings has been demonstrated. [11] We extend this technique to the femtosecond range. We have developed simulation codes to project the group velocity dispersion (GVD) associated with these elements. We will measure the actual GVD, compare it to our simulations, and refine our model if necessary.

Three features of our proposed design help in generating stretching ratios larger than previously reported: (i) our design calls mostly for high gain materials. This considerably reduces the overall amount of material present in the laser path. (ii) In addition we will be working around 1550-nm, a spectral region where most GVD is low. (iii) The finite size of the optical elements found in standard stretchers truncates the bandwidth, imposing limits on the stretching ratio. The use of fiber Bragg gratings will alleviate this problem.

Task 1 - Phase I Results:

We had originally thought of addressing this task starting with a standard CPA implementation and optimizing it for the unique parameters of fiber laser design. One of the key points to be addressed in that context was bandwidth reduction (gain narrowing) during

the amplification process. Our fiber oscillator can produce large bandwidth (>40 nm). It is difficult to maintain this bandwidth during the amplification process. Erbium-doped fiber has a rather unusual wavelength dependent gain, with a strong peak centered around 1530 nm, followed by a flat tail extending beyond 1580 nm. Erbium is also a three-level system. This further complicated the gain narrowing issue by making the gain wavelength dependence a function of the pump power. The telecommunication industry faces the same problem. They have addressed it by introducing gain-flattening Bragg gratings in their fiber system. While this approach works for the telecommunication system, it is not acceptable for us. It introduces significant losses (the gain is flattened by introducing wavelength dependence loss!) and the gain wavelength dependence cannot be readily adjusted for shift in pump power level.

While gain narrowing still remains an important issue we found, during this Phase I, two new ways to alleviate it:

(a)   We learned to generate significant bandwidth at the end of the amplification process. We tested two compression techniques that, not only shorten (compress) the pulse, but also generate extra bandwidth. Because this bandwidth is generated at the very end of our laser system, it is not affected by gain narrowing. Task 2 will present these compression techniques in details.

(b)   We learned to design fibers where we have good control of the group velocity dispersion (GVD). With our latest designs we can independently control the second and third order dispersion term. We had never been able to do so in the past. The availability of this additional adjustable factor will provide for new CPA designs, calling for shorter fiber length, and/or a larger set of active fibers. Using this additional degree of freedom we should be able to reduce gain narrowing during the amplification process. Task 1a will present this engineered GVD technique.

The potential of these two discoveries has not yet been fully explored. This will be pursued in our Phase II. We can now think of very different ways of generating energetic, ultrashort pulses from fiber lasers.

For example we may want to use a relatively narrow linewidth oscillator, combined to a fiber stretcher with tailored GVD. With the proper GVD we should be able to stretch the narrow bandwidth pulse sufficiently to avoid non-linear problem, yet avoid gain narrowing. (Gain narrowing is not only a problem because it prevents the generation of short pulses, it is

9

also a significant source of loss, which we want to avoid even if we are capable of generating bandwidth at the end of our system.)

In summary, while stretching ratio is still clearly an important parameter that needs to be optimized, we now have techniques at our disposal that open up numerous ways to optimize this ratio. Most important, we are not forced to work from the onset with large bandwidths, rather we can design an efficient and robust front-end, and use bandwidth generation techniques at the back-end.

TASK 1A: Group velocity dispersion characterization

Phase I Task Definition:

In order to complete Task 1 we need to characterize the GVD of the various fiber devices employed. While the GVD of standard (passive) communication fiber is generally available from the fiber manufacturers, the GVD of active (Erbium-doped) fibers, or polarization-maintaining fibers is usually not characterized. We will design a system to measure the GVD of these fibers and devices using the technique of spectral interferometry. In this technique the pulses from a broadband source, such as our commercial fiber laser, are split into two replicas one of which travels through the dispersive device to be tested. The two pulses are combined in a spectrometer and the resulting interference pattern can be analyzed to yield the dispersion of the tested device.

Task 1A - Phase I Results:

Task 1A was expanded much beyond our initial proposal. We developed early in our program the GVD measurement technique described above. In order to measure third-order terms we needed a good signal to noise ratio. This was obtaining by upgrading our data acquisition systems. Once this was done we were able to collect the desired data.

In addition as mentioned under Task 1 we developed a way to control independently the fiber GVD second- and third-order terms. Using commercial software we computed GVD for numerous fibers including fiber with depressed cladding (see Figure 4). This unusual design gave us a way to control independently the fiber GVD second- and third-order terms by adjusting the depth of the depressed cladding. This is a very important capability that will be most useful in CPA designs. Being able to control independently second and third order in the stretching would allow us to a use a large range of compression techniques, providing ultimately for higher peak power and shorter pulse duration.

To test this approach we approached RedFern, a specialty fiber manufacturer based in Australia. Together we designed and manufactured depressed cladding fibers and measured their GVDs. The initial fiber runs fell short of our optimum design. The design calls for very small diameter core. The manufacturer did not have the appropriate on-line equipment to measure this parameter during the pulling. We had to resort to pulling a few experimental runs for calibration purposes. We progressively closed onto the desired parameters, and we were able to match our experimental results with our theoretical predictions. To amplify the effect and simplify the testing we even work around 775-nm, a region which is very far from the zero GVD region. This work is ongoing. RedFern is pulling additional runs for us. We expect to meet all of our design objectives within a few months, and we should have this technique well under control for Phase II of this program.

Figure 4: Typical cross section (index profile) of a depressed cladding fiber

Refractive Index Profile
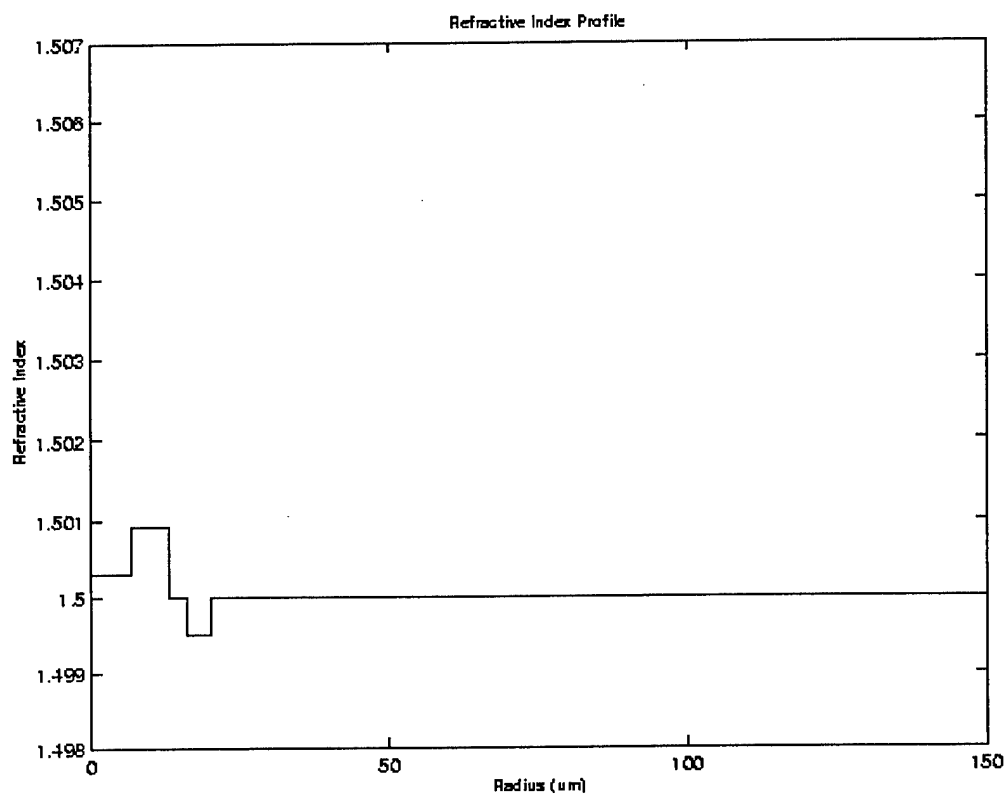
TASK 2: Reduce the pulse duration

Phase I Task Definition:

Our commercial fiber lasers can generate pulses with a bandwidth exceeding 60 nm. This should be sufficient to support pulses shorter than 40 fs. Yet we are presently not able to reach this ultrashort pulse duration. Our pulses are not Fourier-transform limited. We will characterize the pulses using auto-correlators and/or FROG and optimize the overall system to compensate for any non-linear phase chirp, in order to obtain pulses that are Fourier-transform limited.

Gain narrowing in the fiber pre-amplifier is another phenomenon that can reduce the bandwidth and produce long pulses. We will study gain narrowing throughout our laser system. We will develop a code to simulate gain narrowing, and test various ways of defeating gain narrowing. Several products that have only recently been commercially available will help this process: in-fiber gain flattening devices can be used to compensate for gain narrowing; and very wide gain silicate erbium-doped fiber can be used to lessen the gain narrowing (which is becoming an issue in the communication industry). Finally once those elements have been characterized we will optimize the gain distribution among the various subsystems (oscillator, preamplifier and maybe amplifier) to minimize the overall gain narrowing.

Task 2 - Phase I Results:

Two new approaches were studied during our Phase I: Non-linear Raman Soliton Compression; and compression based on Cascaded Chi-2 non-linearity. Both approaches are reviewed below.

Raman Soliton Compression

Fiber-Raman solitons have been extensively studied both theoretically and experimentally because of their fundamental and technological importance.[12] Raman solitons have been observed in fiber amplifiers as well as passive fiber transmission lines. In general, Raman generation in fibers, utilized as a pulse source or as an amplifier, serves to extend the telecommunication window beyond the traditional erbium gain bandwidth ($> 1.56\mu m$).

Raman pulse compression or Raman soliton generation can be understood by first considering Soliton compression itself (Figure 5A). The soliton represents a balance between non-linearities and dispersion. In optical fibers, the non-linearity is associated with an intensity dependent index of refraction giving rise to a nonlinear phase shift through self phase modulation (SPM). In the absence of dispersion, SPM does not affect the temporal pulse envelope but induces bandwidth generation in the form of a positive frequency sweep

13

or up-chirp. If the pulse is propagating down a fiber with anomalous dispersion (negative group velocity dispersion (GVD)), the spreading of the different frequency components that would otherwise cause the pulse width to increase with a down-chirp induces the pulse to decrease in temporal width until the balance is established. At this point the pulse propagates undistorted if it is a fundamental soliton given by the parameter ratio

$$N^2 = \gamma P_o T^2 / |GVD| = 1$$

or undergoes a recurrent pulse shape change for a higher order soliton ($N >= 2$).

The Raman-soliton compressor can be understood by following the diagram in Figure 5B. In our application, an energetic chirped-pulse from the fiber power amplifier (referred to as the pump pulse) is introduced into a negative GVD fiber. This pulse is up-chirped so it undergoes temporal compression as it propagates in the negative GVD fiber. Initially the pump pulse is very broad making its peak power below the nonlinear threshold. As the pulse compresses, the nonlinear threshold is reached and the pulse starts to generate bandwidth through SPM. The Raman gain spectrum in silica fibers is very broad and peaks at a frequency shift of 13 THz. Therefore, once this initial narrow pump pulse spectrum reaches, say, ~10 THz, (roughly the bandwidth supporting a 100 fs pulse), the short wavelength spectral components will feed the long wavelengths via a stimulated Raman process. This stimulated Raman downshift or Stokes generation is referred to as the pulse self-frequency shift. These newly generated Stokes components reflected in the spectrum as a long low frequency tail or a broad low frequency peak (depending on conversion efficiency) migrate to the trailing edge of the pump pulse. In so doing, the energetic pump pulse, still undergoing compression, induces a nonlinear phase shift on the Raman component through cross phase modulation (XPM). Thus in much the same way that the normal soliton forms, the Raman-soliton arises from the balance of negative GVD and XPM from the pump pulse.

Under the right conditions, the conversion from pump pulse to Raman-soliton can be nearly complete. At some point in this energy exchange, the Raman-soliton acquires enough energy to sustain itself through balancing SPM and negative GVD.

FIGURE 5A: Nonlinear Soliton Compression

This phenomenon is based on a balance of self-phase modulated induced "up-chirp" with a GVD induced "down-chirp". Figure 5A shows the fundamental order soliton. The pulse duration evolution is shown above the time axis and the corresponding spectra are shown below the time axis.
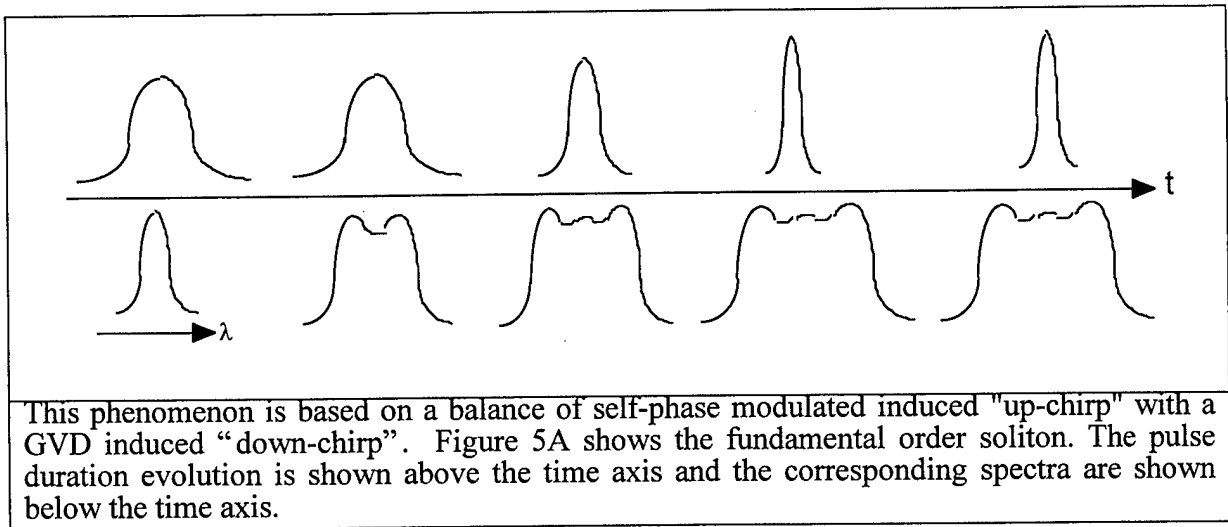
FIGURE 5B: Nonlinear Raman Soliton Compression

This phenomenon is based on a balance of pump induced cross-phase modulated "up-chirp" with a GVD induced "down-chirp". Figure 5B shows the fundamental order soliton. The Pump pulse and the Raman pulse evolution are shown above the time axis. The corresponding Raman spectra are shown below.
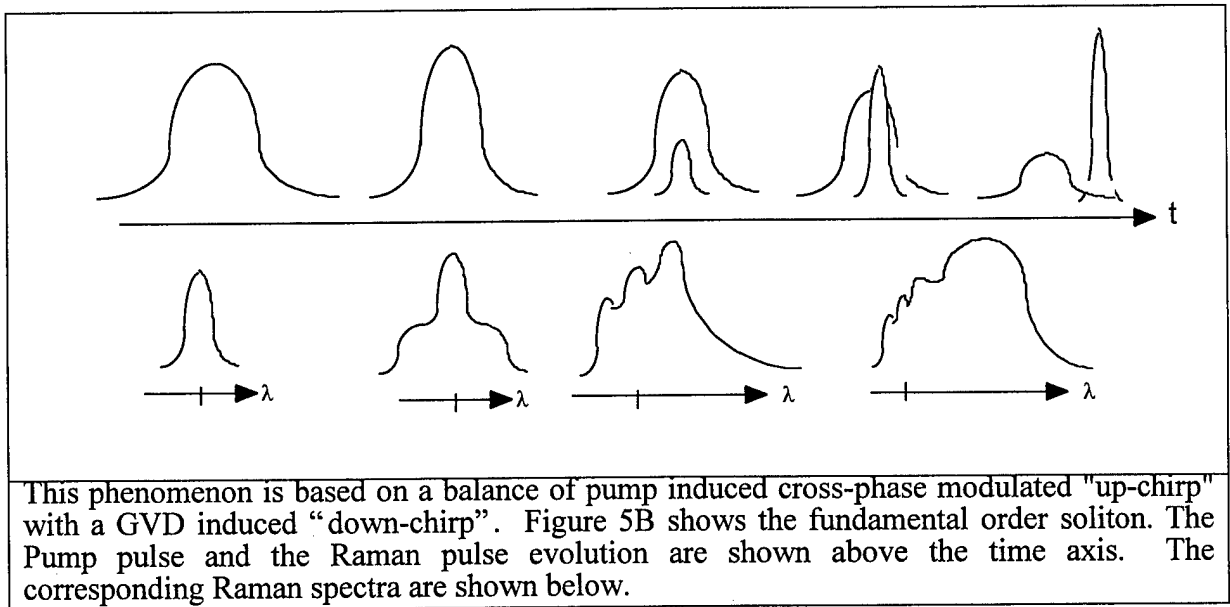
In Phase I of this program, we demonstrated this compression technique (see Figure 6) where a 1.6 μJ input pulse with duration of 350 ps (centered at 1.56 μm) generated a 55-fs pulse (autocorrelation width 88fs) at 1.6 micron. By optimizing the fiber length and pump pulse energy, we were able to achieve at least 65% conversion efficiency corresponding to approximately 1 μJ pulse energy in this short pulse.

FIGURE 6: Nonlinear Raman Compression. Experimental Data

Shown at the very top above is the input pulse. Then shown sequentially for progressively larger amplification (higher energy) are the output spectra. Note the progressive Raman shift to longer wavelength.	Autocorrelation traces corresponding to the spectra showed on the left. At the lowest energy setting the peak power was not sufficient to reach the nonlinear Raman regime. No compression occurred. The pulse durations shown are AC values. True pulse width is approximately 50 % shorter.

In Phase II, we propose improving the conversion efficiency and power scaling of this compression technique. Several factors may be important in improving conversion efficiency. Due to the difference in carrier frequencies, temporal walk-off between the pump pulse and Raman pulse occurs limiting the interaction length. Along the same theme of dispersion allocation in soliton transmission lines (effecting an average soliton), fibers of opposite

dispersion (+GVD) can be fused in-line allowing the Raman pulse to overlap the pump pulse. In fact, positive GVD, Er-doped fibers can be used to provide gain to the residual pump pulse for further energy exchange. Also, the use of fiber Bragg gratings as reflectors for both the pump and Raman fields can be fused in-line at the appropriate separations to effect temporal overlap for a second (or multiple) pass through the compressor fiber.

Besides temporal walk-off, polarization walk-off between the two fields weakens the interaction. Both process, XPM and stimulated Raman scattering, are strongest when the interacting fields are of parallel polarization and weaken by as much as a factor of 3 for orthogonal polarizations. We propose to remedy this by going to all polarization maintaining fiber compressor and post amplifier.

In terms of our nonlinear Raman-soliton compressor, the few cm long large area rigid fibers manufactured to-date do not make for the several meter long negative GVD fiber needed to establish the short pulse formation in our Phase I. We will have to develop transverse direct-writing techniques to manufacture much longer rigid-fibers. Note that these rigid-fibers can be made from bulk phosphate glass, which has an enhanced Raman gain over that found in silica glass. This allows for shorter lengths needed to affect the energy exchange from the pump pulse to the Raman pulse. (Phosphate fibers have been manufactured but are no longer commercially available. We are talking to two fiber suppliers -RedFern and HOYA- to see if they can produce this fiber for us.)

Finally, the dispersion magnitude |GVD| of the rigid-fiber can be supplemented by the direct writing of chirped fiber Bragg-gratings.

In all, nonlinear Raman-soliton compression at the GW peak power level should be feasible with the present state-of-the-art fiber fabrication capability using new designs for large area low NA fibers. At the Terawatt level, new designs and fabrication techniques for significantly larger mode areas will be called upon. In particular, direct-writing micromachined rigid-fibers and photonic crystal fibers shows the most promise at this stage (See Tasks 4 to 7).

Besides the Raman-soliton compressor, the cascaded chi-2 compression technique shows great promise and may be better suited for the Terawatt level peak powers.

Cascaded Chi-2 Compression

Cascaded phase-mismatched second-order process, $\chi^{(2)}(\omega: 2\omega, -\omega)$ is a phenomenon that can provide pulse width compression for high-energy pulses.[13] The technique is conceptually simple (a more formal description is given below): an optical beam traverses a second harmonic generation (SHG) crystal that is rotated off the phase-matching angle (this is the exact opposite of the conditions deemed desirable for second harmonic generation). As

the input pulse propagates through the SHG crystal some of its energy is upconverted to the second harmonic. The efficiency of the process is very low as the crystal is not phase angled properly for doubling. Quickly the conversion saturates. This process reverses and the weak second harmonic beam is downconverted to the fundamental. This process is associated with a slight phase shift, which causes an increase in bandwidth. (The bandwidth growth slightly on the phase matching condition.) The upconversion followed by a down conversion process is repeated many times (thus the name "cascaded"). Overall a net negative phase shift is obtained. This results in a frequency chirping of the optical pulses. This frequency chirp can be easily compensated for by propagating the beam through bulk optical material.

The cascade compressor only requires two optics: the SHG crystal, which provides a negative phase shift and additional bandwidth, and the bulk material that provides positive GVD. As a result this pulse compression scheme is very robust, and efficient.

The theoretical basis of the cascade compressor can be described by starting from Maxwell's equations and applying the rotating-wave approximation. The equations governing the interaction of the fundamental (E_1) and second harmonic (E_2) fields within the SHG crystal are thus given by:

$$\frac{\partial}{\partial z} E_1 = iE_1^* E_2 e^{i\Delta kz} + i2\pi(n_2 I_0)\frac{L_{NL}}{\lambda}\left[|E_1|^2 + 2|E_2|^2\right]E_1 \tag{1}$$

$$\left(\frac{\partial}{\partial z} + \frac{L_{NL}}{L_{GVM}}\frac{\partial}{\partial t}\right)E_2 = iE_1 E_1 e^{-i\Delta kz} + i4\pi(n_2 I_0)\frac{L_{NL}}{\lambda}\left[2|E_1|^2 + |E_2|^2\right]E_2 \tag{2}$$

where Δk is the phase mismatch, the initial intensity is given by $I_0 = \dfrac{\sqrt{\frac{\varepsilon}{\mu}}|E_0|^2}{2}$, λ is the

fundamental wavelength, $L_{NL} = \dfrac{n\lambda}{\lambda\chi^{(2)}E_0}$ is the nonlinear interaction length, and

$L_{GVM} = \dfrac{c\tau_0}{n_{1g} - n_{2g}}$ is the temporal walk-off length between the fundamental and second harmonic with group indexes n_{1g} and n_{2g} respectively. It has been shown that the nonlinear phase shift can be approximated as:

$$\Delta\Phi^{NL} \approx -\frac{\Gamma^2 L^2}{\Delta kL} \sim -I_0 L\frac{(d_{eff})^2}{GVM} \tag{3}$$

with $\Gamma = \dfrac{\omega d_{eff}|E_0|^2}{c\sqrt{n_{2\omega}n_\omega}}$ and L is the crystal length.[14] From this equation it can be seen that the nonlinear phase shift is proportional to the input intensity and the square of the crystal length. It should also be noted that the sign of Δk determines the sign of the nonlinear phase shift

making it possible to work at both positive and negative phase shifts. In general, it is more desirable to work with negative phase shifts in order to avoid self-focusing which will lead to other nonlinear processes, making the compression more difficult to control.

Equations 1 and 2 show that, when $\Delta k \neq 0$, an oscillatory conversion/back-conversion between fundamental and the second harmonic, occurs as the waves propagate through the SHG crystal. This oscillation results in the fundamental wave accumulating a phase shift as it propagates through the crystal. The accumulated phase shift is generally far from ideal (non-linear) due to the group velocity mismatch (GVM) between the two waves. This problem is compounded by the long interaction length, which is normally on the order of the crystal length.

This problem can be significantly reduced by working at large values of Δk. Under this condition, the back conversion from the second harmonic to the fundamental is nearly complete. The interaction length is no longer on the order of the crystal length, but rather of the conversion and back-conversion cycle that is much smaller. Conceptually we can divide the non-linear crystal in many smaller crystals with the initial second harmonic intensity having returned to zero at the input of each crystal. This significantly reduces the problems associated with the GVM (as we start with a "fresh" unchirped second-harmonic wave at each crystal input). This also reduces the distortion in the accumulated phase shift on the fundamental frequency (as compared to working with smaller values of ΔkL where there are fewer conversion cycles over the crystal length.)

A similar argument can be made for the frequency if we define an acceptance bandwidth, $\Delta \omega$, within which the variation of the nonlinear phase shift is limited to a fraction of its average value. From equation 3 the acceptance bandwidth is defined as $\Delta \omega \propto \frac{\Delta kL}{GVM}$. (This is in contrast to the phase-matched acceptance bandwidth that is only a function of the GVM.) The net result is the generation of additional bandwidth with a well-defined quasi-linear phase that can be easily compressed. Further, by using positive values of Δk where the net phase shift is negative the phase can be corrected using bulk optical material with positive GVD.

The compression process saturates at high intensities. The intensity saturation issue can be eliminated by upcollimation of the optical beam. This approach requires large faced crystals. Ultimately the crystal growing process places some upper limits on this approach. However, it has been demonstrated that arrays of crystals can be used to effectively increase the cross-sectional area, which eliminates the intensity issue.[15]

The crystal length is the only other practical limitation, which can be eliminated using a series of SHG crystals. Dr. Wise suggests that using a series of moderately long crystals

and placing a GVM compensator between each of them should provide higher compression ratios than by using a single very long crystal.

The characteristics of this cascaded Chi-2 compressor make it viable for the compression of very high-energy femtosecond pulses by factors of up to 10 with throughput efficiencies above 90%. This will alleviate some of the problems associated with the amplification of very short pulses to the Terawatt level.

Note also that one can pre-compensate some of the pulse width distortions associated with propagation in air of intense pulses. In that respect the cascaded compressor is an exceptionally versatile tool, able to produce either positive or negative phase shift.

Cascaded Chi-2 compression was first tested by our scientific laser division in Ti:Sapphire lasers. Consequently the data available is for a 775-nm operating wavelength, as shown in Figure 7.

FIGURE 7A: Cascaded Chi-2 Compression at 775-nm, spectrum
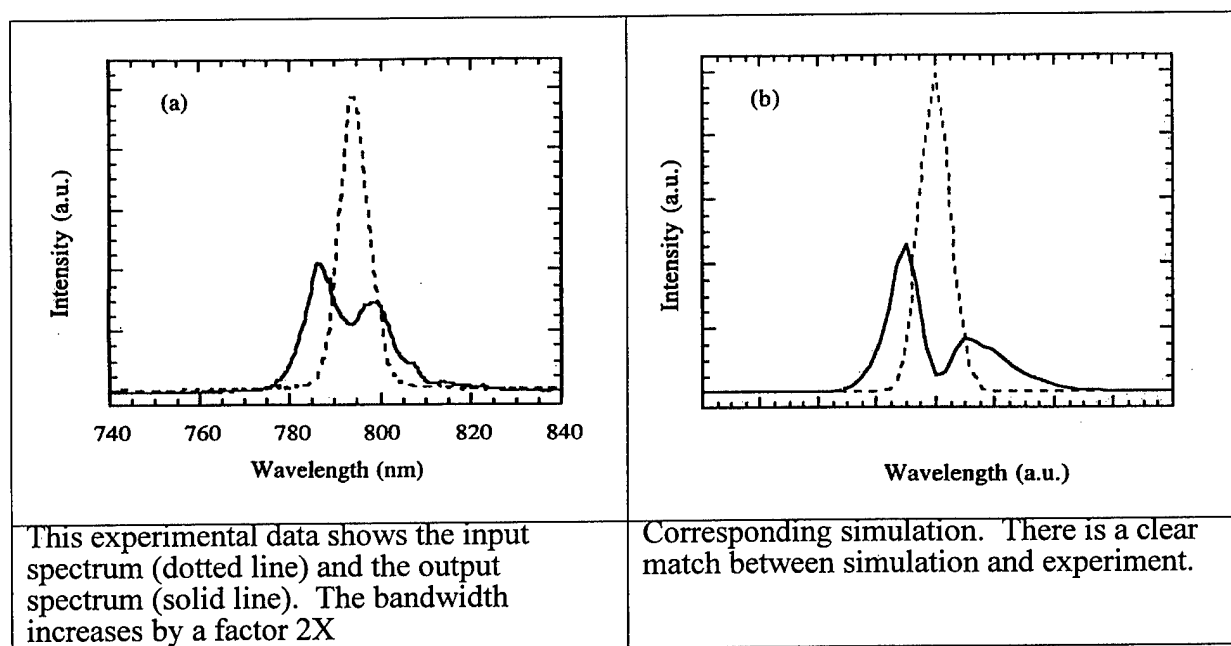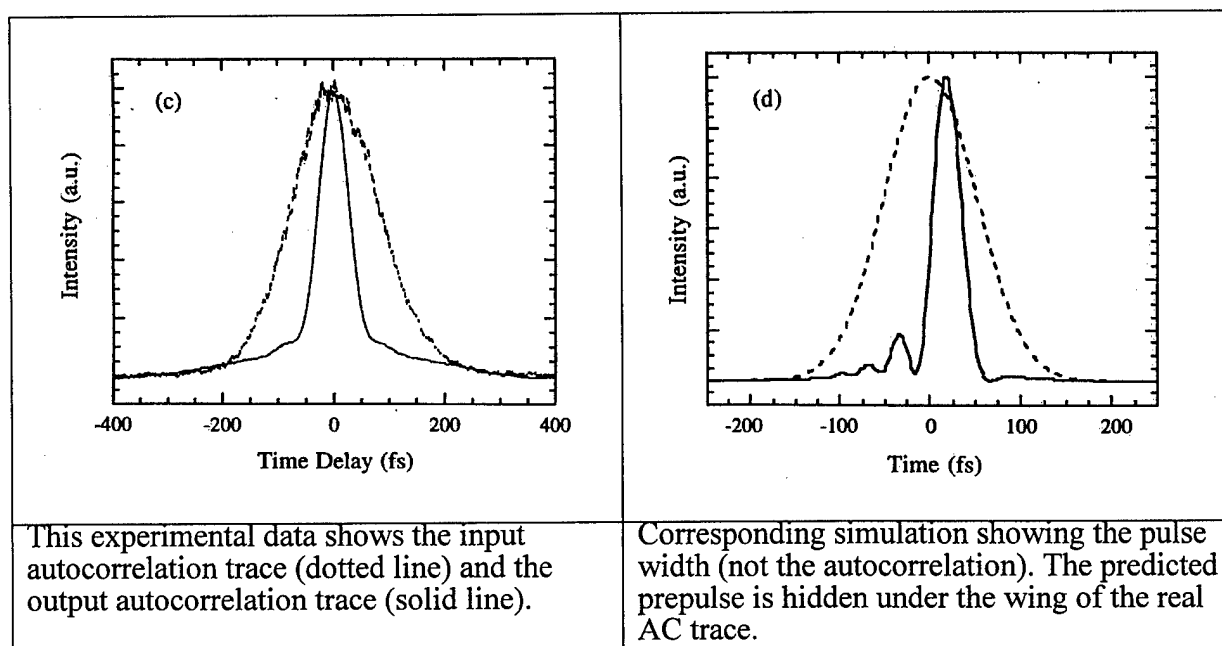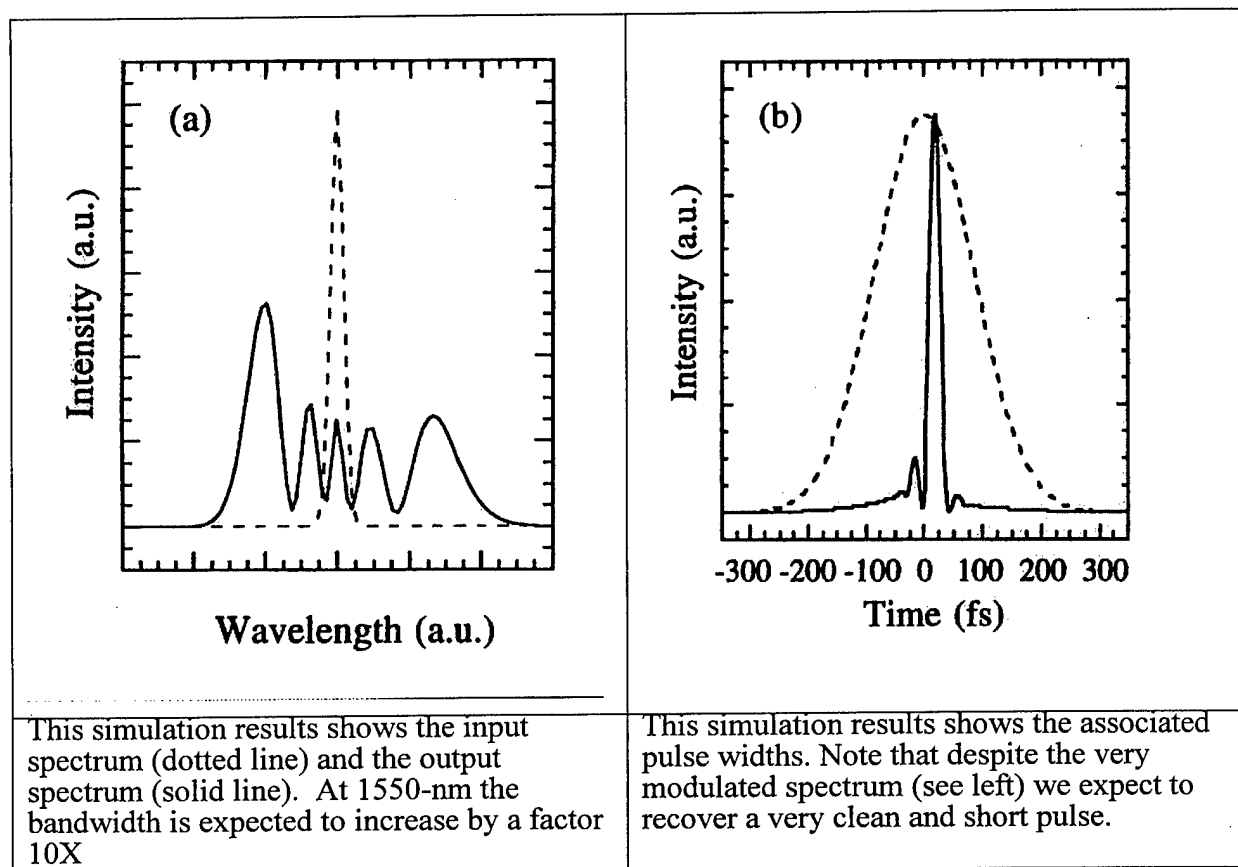

This experimental data shows the input spectrum (dotted line) and the output spectrum (solid line). The bandwidth increases by a factor 2X	Corresponding simulation. There is a clear match between simulation and experiment.

FIGURE 7B: Cascaded Chi-2 Compression at 775-nm, Pulsewidth

(c)	(d)
This experimental data shows the input autocorrelation trace (dotted line) and the output autocorrelation trace (solid line).	Corresponding simulation showing the pulse width (not the autocorrelation). The predicted prepulse is hidden under the wing of the real AC trace.

One of our collaborators, Professor Wise (Cornell University), was able to run some preliminary simulations at 1550-nm. The process is predicted to work very well at 1550-nm as the material GVD is much smaller than at 775-nm. We will be able to use longer input pulse widths and we should get compression ratio of the order of ten. See Figure 8.

(This high compression ratio has not been measured, only calculated. So far we have not been able to test the process at 1550-nm. Our commercial fiber oscillators are not intense enough for Cascaded Chi-2 Compression based on standard bulk non-linear crystals. Using waveguides in PPLN should provide interaction length sufficiently long to reach threshold. Dr. Wise's group is working on demonstrating this implementation.)

FIGURE 8: Cascaded Chi-2 Compression at 1550-nm, Spectrum and Pulsewidth

 Wavelength (a.u.)	 **Time (fs)**
This simulation results shows the input spectrum (dotted line) and the output spectrum (solid line). At 1550-nm the bandwidth is expected to increase by a factor 10X	This simulation results shows the associated pulse widths. Note that despite the very modulated spectrum (see left) we expect to recover a very clean and short pulse.

In summary, the Cascaded Chi-2 Compression approach is generally stable as it relies on saturation of a non-linear effect. It has the potential to handle high average power. Note that this process requires a relatively short pulse width to start. This shortcoming may be partially eased at high peak power. This Cascaded Chi-2 Compression process provides extra bandwidth. Professor Wise has suggested that a two-stage approach may lead to the generation of extremely short pulses (less than 10 fs). Cascaded Chi-2 Compression is compatible with energetic pulses (and high average power) as spatial lateral extend is essentially unconfined, except for the size non-linear crystal. Even this limitation may be lifted with crystal arrays. Finally, we should point out the extremely high efficiency (>90%) associated with this process, as well as preservation of high spatial mode quality.

Compression: a comparison

The two compression approaches tested in Phase I were unexpected. They are not listed under any of the Phase I tasks. Cascaded Chi-2 compression was first tested by our scientific laser division in Ti:Sapphire lasers. Consequently the data available is for a 775-nm operating wavelength. We do not yet have a full understanding of the respective

capabilities and limitations of these compression approaches. Table 2 summarizes what is known at this point. Both techniques will have to be further evaluated in our Phase II. This is our Task 1C.

For the time being, lets say that both compressions work well. Both provide extra bandwidth. This removes the significant constraint of preserving the pulse bandwidth through the fiber amplifier chain. We may even consider starting with a much narrower picosecond FT-limited pulse to avoid a lot of the amplifier complexity, increase the efficiency, and allow more use of standard telecommunication components (these components usually have much narrower bandwidth than what is called for by our femtosecond sources)

Our Phase I did call for a compressor, but it was of a very different type. It serves a simpler function: to compensate for the stretching we had imposed on the pulse upfront. We had accepted the fact that the compression would have to be done with a grating-type compressor, which was the weakest point in our Phase I approach. The recent developments in compression technology give us the opportunity to address this issue with other, more robust solutions.

TABLE 2: Comparison between Nonlinear Raman Compression and Cascaded Chi-2 Compression

	Nonlinear Raman Compression	Cascaded Chi-2 Compression
Operating wavelength	Tested at 1.55 micron	Tested at 775-nm. Simulated at 1.55 micron
Compression ratio	> 1000X demonstrated	3 X demonstrated at 775-nm 10X expected at 1550-nm Higher ratio reachable with two-stage design
Generate additional bandwidth?	Yes	Yes
Maximum input pulse duration	300 ps demonstrated	1 ps at 1550-nm in a single stage
Minimum output pulse duration	50 fs at 1550-nm demonstrated during Phase I	60 fs at 775-nm demonstrated during Phase I
Average power capability	To be studied in Phase II	To be studied in Phase II.
Peak power capability	10 TW/cm2 demonstrated during Phase I	10 GW/cm2 demonstrated during Phase I
Beam quality	Excellent	Good

23

TASK 3: Fiber-based front-end

Phase I Task Definition:

With the results of Tasks 1 and 2 at hand we will design a complete fiber-based front-end including a fiber-oscillator, fiber stretcher, fiber preamplifier (and maybe depending on the results of Task 2) a fiber amplifier (See Figure 3). The design will optimize for compactness and robustness.

The same front-end will be used in the Phase II of this program to seed the macrowaveguide-based final amplification stage(s). Note that when fitted with a compressor this front-end may be of interest for numerous related applications. For example it would make a very compact and very reliable ultrafast pump source for femtosecond OPAs and THz sources.

Phase I Results:

Toward the ends stated in task 3, a fiber-based pulse stretcher / preamplifier / power amplifier was built during Phase I. This device went through several reconfigurations. We are reporting here only the most salient features.

As it stands, the output of our fiber oscillator ($\sim$ 3.5 ps, 60-nm FWHM centered at 1550-nm, compressible to $\sim$110-120 fs) is pre-amplified and stretched in time to 150-200 ps (the pulse length is adjustable with fiber length). Spectral shaping due to the gain and dispersion characteristics of the fibers resulted in a spectrally narrower yet more compressible pulse. This alludes to an issue we briefly mentioned in our Phase I proposal – the spectral chirp produced by our oscillator and our stretcher is highly non-linear. It cannot be fully compressed using standard compression techniques. Reducing the bandwidth, and thus the amount of non-linear chirp, may, under some conditions, provide for shorter compressed pulses. As a seed signal in our amplifier circuit, these initially (multi-ordered) frequency-swept, broad-bandwidth pulses are gain narrow and consequentially linearized in their frequency chirp. Here, the amplified pulses are made more compressible to their transform limit with conventional "linear" compressors (a grating or prism pair represents an ideal compressor for linearly chirped pulses). Being made more compressible to their transform limit, these bandwidth narrowed pulses (10nm – 20nm) can be made no shorter than $\sim$150f (20nm) or 300fs (10nm). Their "quality", however, makes for a better input pulse for nonlinear compression.

Initially we attempted to maintain the oscillator bandwidth through the pre-amplifier and the power amplifier(s). (In the latter stage of our Phase I program we abandoned this approach after developing bandwidth generating techniques as explained above.)

Initially pre-amplification was used to recover the energy losses suffered in the stretcher and in the pulse-picking acousto-optic modulator (repetition rate control) and to provide some signal amplification to better compete against amplified spontaneous emission (ASE).

Pulse stretching was accomplished in three different ways:

1) Using specially design chirped-fiber-Bragg gratings,

2) With engineered index profile fiber for dispersion and dispersion slope control (see task 1A), and

3) With a combination of both fiber Bragg gratings and fiber. The fiber Bragg gratings used in 1) and 3) were designed for broadband reflection (60+nm) and pulse stretching from ~ 100fs to ~250ps. Though the reflectivity profile and induced frequency chirp (determined via spectral interferometry) agreed quite well with the test design, amplification of these stretched pulses resulted in high frequency modulations in the amplified spectrum. These spectral modulations are most likely due to phase irregularities from apodization errors. A redesign of the fiber Bragg gratings for narrower bandwidths (~20-25nm) was considered, but not pursued due to budget constraints.

Pulse stretching with fiber only (to ~150 ps) and subsequent amplification did not show these high frequency spectral modulations yielding a much cleaner amplified spectrum. Dispersion control by specially designed fiber index profile does not offer the flexibility in design as with fiber Bragg gratings. However, if one is interested in narrower bandwidth amplification and subsequent recompression to, say, picosecond pulse durations, then multi-order dispersion control is less significant. (See task 1A)

During the course of our Phase I (pre)-amplification has been performed with standard TELECOM erbium doped fibers. These fibers are by no mean optimum for our designs. They have been optimized for small signal gain efficiency and not energy storage capability. (The latter is called for in this application.)

In the early part of our Phase I we were able to achieve amplification to the 0.5 microjoule pulse energy level at 500-kHz and the multi-microjoule level at 10-kHz repetition rates. In both cases the major energy limitation was amplifier self-saturation through ASE.

To confront this limitation, two steps were taken. In one case both gain flattening and ASE filters are being incorporated into the amplifier chain. The other case involves

incorporating large mode area erbium fibers. This second approach is still ongoing. Large core fiber was just produced by RedFern and should be available for the Phase II of this program.

In the second half of our Phase I program we concentrated on suppressing the ASE and increasing the energy extraction from the erbium amplifier chain. We were able to achieve multi-microjoule pulse energies at repetition rates as high as 250 kHz. This again was achieved with commercially available, standard TELECOM erbium fibers, which are optimized for gain efficiency and not energy storage. Both the small mode field diameters and large gain efficiency, characteristic of these erbium-doped fibers, require the input signal pulses to be temporally stretched to several hundred picoseconds in order to minimize nonlinear distortions. Such distortions would compromise the pulse compressibility.

Chirped fiber Bragg gratings where implemented for pulse stretching. Despite adequately achieving the needed temporal stretching factor, the small ripple in their group-delay response (from insufficient apodization) resulted in severe spectral distortion and pulse break-up in the amplified signal even at relatively small pulse energies (10-100 nJ). In place of the fiber Bragg gratings, a fiber stretcher incorporating dispersion compensated fiber (DCF) and a high numerical aperture fiber is being used. While both fibers have normal dispersion (positive group velocity dispersion), the dispersion slope of DCF is opposite (negative) to that of the other as well as that of the erbium-doped fiber and therefore partially compensating for the cubic phase term.

In order to minimize the long fiber lengths needed for pulse stretching with a single pass configuration, a multi-pass geometry incorporating a fiber preamplifier was used during our Phase I. While this approach was found useful for this present work, it is a mechanically weak implementation. We intend to replace this approach with a much more robust engineered fiber stretcher in the Phase II (See task 1A).

With this implementation, microjoule pulse energies where produced at 250 kHz with essentially no measurable amplified spontaneous emission (ASE).

At much lower repetition rates ~1kHz the pump requirement is greatly reduced at the expense of greater competition with ASE. However using a ASE filter which blocks out the major ASE peak at 1536nm and passing 1545nm on (towards longer wavelengths) with <0.5dB loss and shortening the Er-fiber to under 1.5m, the µJ level pulse energies are reached at <200mW pump power (at 980nm). This pump power is achieved with commercially available laser diodes.

Presently our work concentrates on lowering the repetition rate of the amplifier to optimize pulse energy extraction and the recovery of a short (100-150 fs) pulse. Er-fiber optimized for high-energy power amplification has been designed. It involves a depressed

core and a raise cladding index for maximum mode field diameter while maintaining single mode propagation. RedFern has delivered some preliminary samples.

Note that the DCF fiber is no longer commercially available. Due to the explosive need for fiber components generated by the telecommunication industry, we found that several of our suppliers are abandoning marginal product lines to concentrate on highly profitable telecom articles. This trend is worrisome. We are now left with only one reliable specialty fiber supplier (RedFern, based in Australia!). We are trying to establish a relationship with HOYA of Japan, in the hope of having a second source should RedFern be unable to meet our needs.

TASK 4: Micromachining (direct-write) simple waveguides in glass slab

Phase I Task Definition:

Many investigations on the effect of ultraviolet radiation damage (index change) in Ge-doped silica glasses have been performed in order to produce optical devices in fibers and thin-films. On the other hand, laser index change via visible and infrared radiation has received little attention due to the low-photon energy until recently, when Hirato and his colleagues have shown the effect of near-infrared femtosecond pulses on various glasses.[16] Large increases in refractive index were observed, resulting in the formation of optical waveguides. Most of the previous fabrication methods (vapor deposition or ion exchange) are intrinsically two-dimensional techniques while the multiphoton technique demonstrated by Hirato is three-dimensional. Though it is still in an early stage of development this direct-write technique is very promising for realizing compact all solid-state lasers and amplifiers (See Task 6).

We have partially duplicated the work of the Japanese group and recently delivered waveguides to Corning. We will further improve our glass waveguide writing technology during Phase I.

Task 4 - Phase I Results:

We studied extensively this subject during our Phase I. We used one of our commercial femtosecond workstations to write waveguides in various glasses. While the process is not fully understood we believe the following to generally apply: At the operating wavelength, 775 nm, the glass is transparent to the incident light. In this case the ultrashort laser pulses interact with the glass through the creation of color centers via a multiphoton absorption process. This absorption is followed by a local melt of the glass. The glass later re-solidifies with slightly different physical or/and chemical properties. This gives the glass a larger index of refraction in the area where the femtosecond pulses were applied. Therefore, a beam of light propagating along the same path in the glass will be guided due to total internal reflection, which is caused by the difference in the index of refraction.

We first experimented with a regular glass microscope slide (soda lime glass). The beam was focused in the center of the glass with a 40 mm lens and the sample was translated in a direction perpendicular to the beam axis. Lines were written at various pulse energies. Professor Kim Winick from the University of Michigan characterized the resulting waveguides.

We also worked with soda-lime glass slides and fused silica slides. Energies ranging from 0.3 μJ to 74 μJ were tried. We used either a 40-mm or a 15-mm focusing lens. Writing speeds raged from 25 μm per second to 250 μm per second. As expected under the same

28

operating conditions the lines made in fused silica were thinner than those made in glass (fused silica has a lower non-linear index of refraction).

Professor Kim's group confirmed the waveguiding action. It was found that the waveguides have an elliptical cross-section. This ellipticity is attributed to the focusing beam geometry of the laser (the waveguides were written in the glass in a transverse direction to the beam propagation axis). The ellipticity ratio ranged from 16 to1 at worst to 3 to 1 at best. Although the transverse geometry is of significant interest for the fabrication of long waveguides, we decided for the Phase I to use a longitudinal geometry.

In a second series of experiments we explored the possibilities of writing waveguides along the propagation of the laser beam. The beam was focused in the center of the glass with an 80 mm focal-length lens and the sample was translated in a direction parallel to the beam axis. Lines were written at various pulse energies and with various numbers of scans. After examining the lines under the microscope we could conclude that they have cylindrical geometry. The lines written with high-energy pulses ($25\mu J$-$100\mu J$) appeared to have dark structure in the middle, which we attribute to high-energy damage (cracks, holes, bubbles etc.) However, the lines written with lower energy pulses ($2\mu J$-$10\mu J$) showed no such features and appeared to have very uniform structure under the microscope.

Figure 9: Single-mode waveguide

The waveguide in figure 9 is single mode, supporting only the lowest order mode LP_{01} (at 633-nm). This far-field image illustrates the excellent quality of the waveguide we can fabricate with our direct write technique.
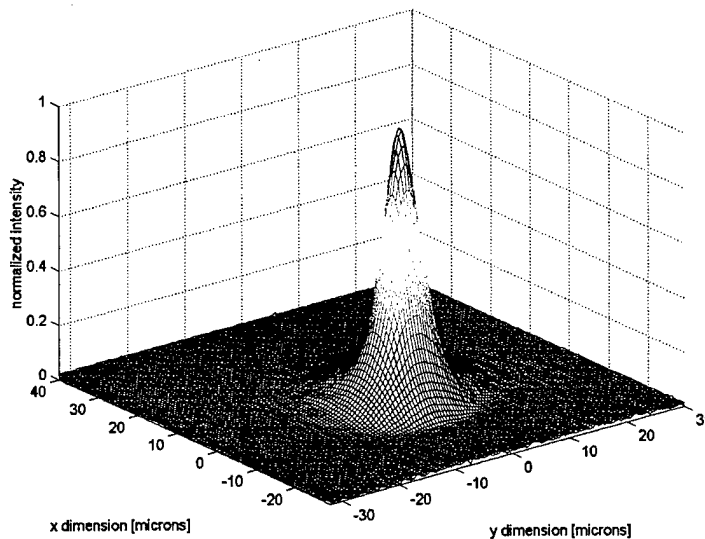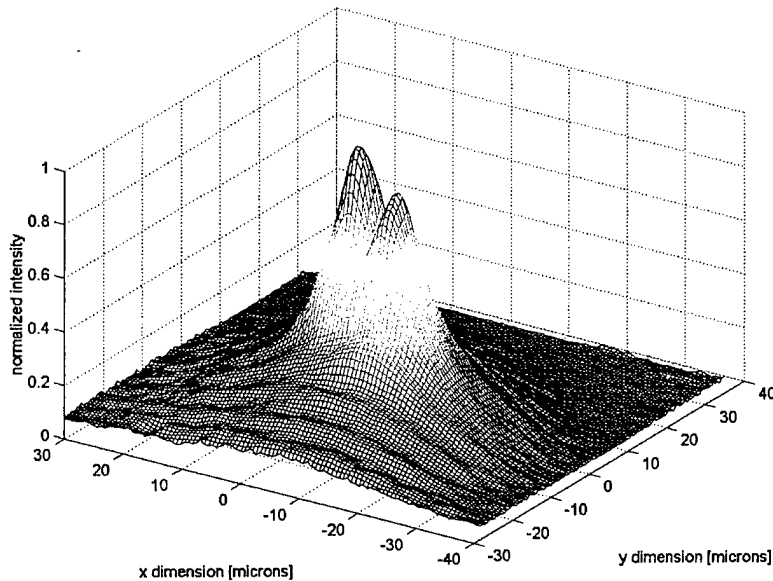

29

Figure 10: Dual-mode waveguide

The waveguide in figure 10 is single mode supporting only the second order mode LP_{11}.

After examining the waveguides under the microscope we couple some HeNe laser light into them. The waveguides written with high-energy pulses had typically a 15-to 30-micron radius (function of the processing parameters) and therefore were easy to couple light into. However the throughput of those waveguides appears to be very low due to very high internal scattering losses. (The light scattered was easily visible by eye.) On the other hand, the waveguides written with pulses of low energy had small cross-sections and therefore were not easy to couple light into, but they showed no visible scattering. Latter tests confirm the high quality of these waveguides.

To further demonstrate the potential of our direct-write technique we fabricated waveguide couplers as shown in Figure 11 and 12.

Figure 11: two to one coupler

We wrote two waveguides located in close proximity to each other. Light was then coupled in the waveguide on the left and progressively coupled to the waveguide on the right. Note that this process has not, so far, been perfected. Some residual light is still found in the original waveguide (this is undesirable). We fabricate the waveguides sequentially. This is probably not a good choice. The manufacturing of the second waveguide is affected by the close proximity of the first waveguide. In other words, if they are close enough to operate as

30

a coupler, they are close enough to affect each other during the fabrication process. Fabricating the waveguides in parallel would eliminate this restriction.
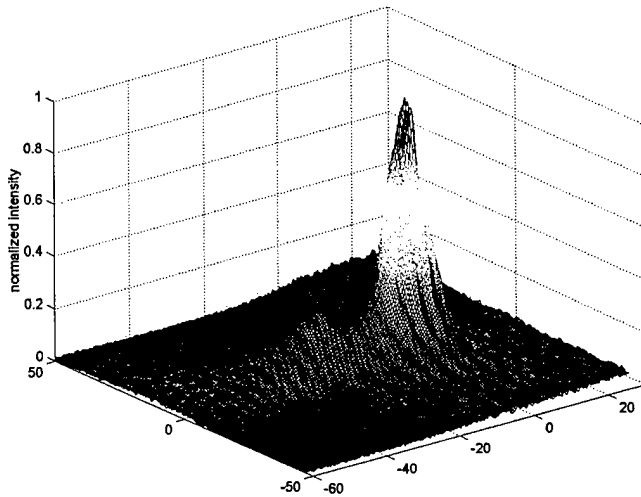

Figure 12: One to four coupler

We wrote four waveguides located in close proximity to each other. Light was then coupled in the waveguide on the right and progressively coupled to the three waveguides on its left. Here again the process has not been perfected. We were trying to equally distribute the energy among the four waveguides. Clearly more work needs to be done to reach that goal.
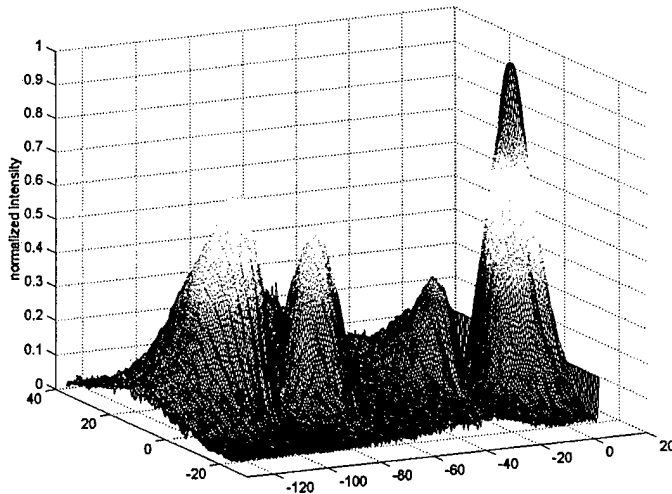
Devices of this kind (and more advanced types) may be used in our Phase II to couple multiple diodes into a single fiber. While average power was not an important factor in our Phase I, we will of course have to address that issue before commercializing our work.

TASK 5: Qualify waveguides micromachined by direct-write

Phase I Task Definition:

We will optically polish the ends of waveguides in glass hosts fabricated under Task 4. We will measure losses and mode profiles of these waveguides, and we will provide feedback to improve micromachining quality and produce low-loss waveguides.

Task 5 - Phase I Results:

The waveguides fabricated under task 4 were tested at the University of Michigan by Professor Kim Winick.

Coupling efficiencies was measured at 633-nm. Single-mode waveguides, as shown in Fig. 9, showed coupling in excess of 25% (this value is uncorrected for surface reflections loss). To measure the internal scattering loss of our single-mode waveguides, we fabricated under fixed operating parameters several waveguides of various lengths. The shortest waveguide was as short as one third of the longest one. Then the transmission of all the waveguides was measured. We did not detect any variation outside our experimental coupling error. We were able to place an upper limit of 1dB/cm on the internal loss associated with our direct-write waveguides.

The waveguides written with the 200 mm focal-length lens at higher energy were larger in diameter (40-50 µm). These waveguides had a transmission of 50 to 60 %. The larger transmission in this case can be attributed to better coupling of light into the waveguides due to the larger diameter. Despite the large diameter of these waveguides, their far field transmission still showed single-mode features.

TASK 6: Micromachining (direct-write) channel waveguide laser in glass slab

Task 6 - Phase I Task Definition:

After successful completion of tasks 4 and 5 we will fabricate a device, such as a channel waveguide laser, using our direct-write technology. We will characterize it (loss, mode profile, gain, etc.).

Task 6 - Phase I Results:

We were able to apply the know-how gained from working with passive glasses to the fabrication of active waveguides (*i.e.* waveguides that exhibit gain). We wrote waveguides in Nd-doped glass. We focused in the bulk of the glass with an 80 mm focal-length lens and the sample was translated in a direction parallel to the beam axis. The scanning was performed such that the waveguide was written starting close to but not on the back surface of the sample and ending close to the front surface. The beam was not focused on either surface of the sample in order to avoid damage to the surfaces. Lines were written at various pulse energies and with various scan speeds.

The waveguide quality was similar to that of our passive waveguides. Scattering losses were too low to be measured with our equipment. The gain was measured around 1.05 micron. To the best of our knowledge these are the first active waveguide ever produced by direct write. These waveguides were tested extensively at the University of Michigan. We reported our results in Electronics Letter, Volume 36, February 3rd 2000, page 226.

To measure the gain of our waveguides we used an Argon-ion pump laser (operating at 514 nm) and a seed signal at 1054 nm. We used a counter-propagating geometry in which the pump beam is launched in the waveguide by end firing through one end. The signal is also end-fire coupled but through the other end. The launched signal power levels were on the order of 300 µW. The signal beam was chopped and the changes were recorded as the pump beam was turned on and off for few different levels of pump power.

The data on the gain of the amplifier at a signal of 1054 nm is presented in Figure 13. The gain was measured as the ratio between the signal power with the pump turned on and the signal power with the pump turned off. The pump power was measured in front of the input coupling objective and preliminary estimates indicate a coupling efficiency of 20 % to 40 %. In order to verify that the change in the signal power is not due to some thermal effects, the experiment was repeated using the 488-nm line of the Argon ion pump laser. The fact that no gain was observed, as expected, since Nd does not have a 488 nm absorption band, ruled out the influence of thermal effects. Fluorescence data indicates that the emission-cross section at 1054 nm is only half as large as that at the 1062 nm peak. Thus this

34

device exhibits a gain of about 3 dB/cm for input pump power levels of approximately 350 mW. This amount of gain should be sufficient to support lasing, provided that high reflectors are affixed to the ends of the waveguide.

Figure 13: Active waveguide fabricated by direct-write

Signal gain versus input pump power
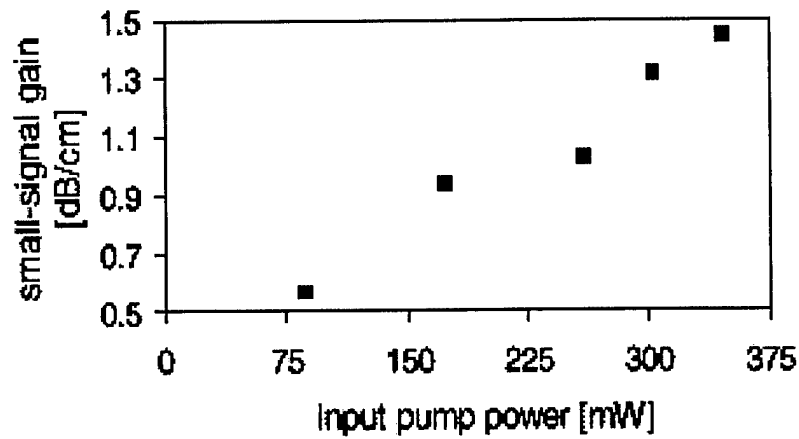
Experiments to achieve lasing are still in progress. We will also perform a more extensive characterization of these waveguide devices, including more accurate loss measurements and a thermal stability study.

TASK 7: Analyze impact direct-write for macrowaveguide generation

Task 7 - Phase I Task Definition:

Very large waveguides, and photonic crystal fiber (PCF) will play an important function to reach high-energy levels. These devices have only rarely been used in laser design. The few PCFs manufactured so far have been passive devices. We are proposing to develop active devices with substantial gain. While passive devices may play a role in femtosecond laser design (for compression?), active devices are going to be much more important. We will place special emphasis on waveguides manufactured through the direct-write approach. Already it is clear that the direct-write approach has some advantages, and some disadvantages over the pre-form approach. For example the direct-write technique is expected to be compatible with numerous host materials, while the pre-form approach is designed for glass hosts. On the other hand the waveguide length is going to be more limited in the direct-write approach than in the pre-form approach. High-doping level (high gain) may mitigate this drawback.

We will study how to pump macrowaveguides. We have already mentioned that PCFs are intrinsically single-mode at all wavelengths (for which the substrate is transparent). This allows for long co-propagation of the pump energy and signal energy, resulting in higher efficiencies. Efficiencies may be further increased (over conventional designs) as waveguides manufactured in slab offer an unusual active volume over cooling surface ratio.

Finally we will study the possibility of designing femtosecond lasers that use only waveguides (*i.e.* no fibers).

Phase I Results:

Based on the results of this Phase I we have placed on-hold the idea of developing femtosecond lasers based only on macrowaveguides. Rather we intend to push conventional fiber front-end to the 0.1 to 1 GW level using large core fibers for the power amplifier stages. We have gained considerable experience designing specialty fibers during our Phase I, have developed tools to characterized these fibers, and have found a good manufacturer. Consequently we will push this approach to the maximum extent possible in our Phase II. We will still used direct-write fabrication to create novel, efficient ways to couple light into the fiber(s), to potentially manufacture power amplifier booster stages (operating at the very end of our amplifier chain). We will also look at the use of ultra-wide waveguides as bulk compressors.

We found that we are able to make waveguides that have very high transmission. We also determined that we could make multimode or single mode waveguides depending on the laser parameters and focusing geometry. For a given laser spot size, we could write a single

mode waveguide of different orders by changing the laser pulse energy. We also demonstrated more complex waveguiding structure such as coupler. This experience gained during our Phase I is unmatched in the industry. It will be invaluable in the manufacturing of the waveguides called for in our Phase II.

Conclusions

In summary, we met our Phase I objectives. We demonstrated a high peak-power ultrafast fiber laser. We invented new way of generating under controlled conditions additional bandwidth, thus defeating gain narrowing. We showed a novel way of controlling second and third order GVD in fibers. We developed a unique capability to direct write waveguide in glass. Commercially we were successful at attracting third-party funding. We are actively developing programs and searching additional funding for the early commercialization of the direct-write technology partially developed under this Phase I. We are also actively searching partners to further develop and commercialize fiber lasers. We believe these exceptional results fully justify Phase II funding for which we have applied.

Literature Cited

[1] Y. Sikorski, A.A. Said, P. Bado, R. Maynard, C. Florea, K.A. Winick, Electronic Letters, Vol.36, No.3

[2] G. Agrawal, Nonlinear Fiber optics (Academic press, San Diego, 1995) ch. 4.

[3] D. Strickland and G. Mourou, Opt. Comm., **56**, 219 (1985).

[4] P.Maine, D. Strickland, P. Bado,M. Pessot, and G. Mourou, IEEE J. QE, **24**, 398, (1988).

[5] K. Tamura, E. P. Ippen, and H. A. Haus, Appl. Phys. Lett. **67**, 158, (1995).

[6] A. Galvanauskas, SPIE Vol. 2377, 117, (1995).

[7] C.P. Barty *et al.* , Ultrafast Phenomena X, 77, Ed. P. Barbara *et al.* Springer, (1996).

[8] A. Galvanauskas, Opt. Lett. **22**, 105, (1997).

[9] D.J Richardson *et al.* , Opt. Lett. **23**, 1683, (1998).

[10] M. Hofer, M. E. Fermann, A. Galvanauskas, D. Harter, and R. S. Windeler, Opt. Lett, **23**, 1840, (1998).

[11] A. Galvanauskas, P. A. Krug, and D. Harter, Opt. Lett, **21**, 1049 (1996).

[12] Govind P. Agrawal, Nonlinear Fiber Optics, 2nd ed. Academic press. Chap. 8, 1995.

[13] X. Liu, L. Qian, and F. Wise, Opt. Lett., **24**, 1, (1999).

[14] R. Desalvo, D.J. Hagan, M. Sheik-Bahae, G. Stegeman, and H. Vanherzeele, Opt. Lett., **17**, 28 (1992).

[15] W. Smith et al. LLNL Report 94-536A

[16] K. Miura, Jianrong Qui, H Inoyue, T. Mitsuyu, and K. Hirato, Appl. Phys. Lett. **71**, 3329, (1997).

DISTRIBUTION LIST

DTIC/OCP
8725 John J. Kingman Rd, Suite 0944
Ft Belvoir, VA 22060-6218   1 cy

AFRL/VSIL
Kirtland AFB, NM 87117-5776   2 cys

AFRL/VSIH
Kirtland AFB, NM 87117-5776   1 cy

Clark-MXR, Inc.
7300 W. Huron River Dr.
Dexter, MI 48130   1 cy

Official Record Copy
  AFRL/DELS/Dr. L.A. Schlie   3 cys